PALEOCEANOGRAPHY, VOL. 28, 599–606, doi:10.1002/palo.20038, 2013

Agulhas salt-leakage oscillations during abrupt climate changes of the Late Pleistocene

Gianluca Marino,[1] Rainer Zahn,[1,2,3] Martin Ziegler,[4] Conor Purcell,[4,5] Gregor Knorr,[4,5] Ian R. Hall,[4] Patrizia Ziveri,[1,6] and Henry Elderfield[7]

Received 5 June 2013; revised 19 June 2013; accepted 24 June 2013; published 2 August 2013.

[1] An ensemble of new, high-resolution records of surface ocean hydrography from the Indian-Atlantic oceanic gateway, south of Africa, demonstrates recurrent and high-amplitude salinity oscillations in the Agulhas Leakage area during the penultimate glacial-interglacial cycle. A series of millennial-scale salinification events, indicating strengthened salt leakage into the South Atlantic, appear to correlate with abrupt changes in the North Atlantic climate and Atlantic Meridional Overturning Circulation (AMOC). This interhemispheric coupling, which plausibly involved changes in the Hadley Cell and midlatitude westerlies that impacted the interocean transport at the tip of Africa, suggests that the Agulhas Leakage acted as a source of negative buoyancy for the perturbed AMOC, possibly aiding its return to full strength. Our finding points to the Indian-to-Atlantic salt transport as a potentially important modulator of the AMOC during the abrupt climate changes of the Late Pleistocene.

Citation: Marino, G., R. Zahn, M. Ziegler, C. Purcell, G. Knorr, I. R. Hall, P. Ziveri, and H. Elderfield (2013), Agulhas salt-leakage oscillations during abrupt climate changes of the Late Pleistocene, *Paleoceanography*, *28*, 599–606, doi:10.1002/palo.20038.

1. Introduction

[2] Rapid changes are a prime expression of the inherently unstable Earth's climate [*Broecker*, 1997]. One notable example of this instability is the millennial-scale and abrupt ocean and climate variability of the Late Pleistocene [e.g., *McManus et al*., 1999; *Pahnke et al*., 2003; *Jouzel et al*., 2007; *Martrat et al*., 2007; *Hodell et al*., 2008; *Charles et al*., 2010; *Barker et al*., 2011] that is commonly ascribed to changes in the strength of the Atlantic Meridional Overturning Circulation (AMOC) [*Broecker et al*., 1990] and of its associated interhemispheric transport of oceanic heat [*Trenberth and Caron*, 2001]. Synchronization of ice core records from both polar regions to a common time scale has shown that these oscillations did not occur synchronously across the hemispheres; that is, the abrupt and high-amplitude temperature shifts in Greenland were out of phase with respect to the gradual changes in Antarctica [*Blunier and Brook*, 2001]. This "bipolar seesaw" [*Broecker*, 1998] is consistent with the contrasting response simulated for each hemisphere to reorganizations of the cross-equatorial heat transport dictated by AMOC strength variations [e.g., *Knutti et al*., 2004] and with the notion that the ocean played a pivotal role in millennial-scale climate fluctuations. Transient AMOC shifts and attendant bipolar seesaw behavior were also recurrent features of the Late Pleistocene glacial-interglacial transitions, with implications for the deglacial exchange of carbon between the deep ocean and the atmosphere [*Cheng et al*., 2009; *Barker et al*., 2011].

[3] Millennial-scale reorganizations of the coupled ocean-atmosphere system are therefore a central component of the Late Pleistocene climate dynamics, but their underlying controls remain elusive, notably for the abrupt switches between cold (stadial) and warm (interstadial) conditions that punctuated the North Atlantic climate during the last several glacial-interglacial cycles [*Martrat et al*., 2007; *Barker et al*., 2011]. *Broecker et al*. [1990] hypothesized that millennial-scale AMOC changes were modulated by salinity oscillations altering ocean water density (buoyancy) in the proximity of the North Atlantic Deep Water (NADW) formation sites [*Renold et al*., 2010]. Freshwater discharge from collapsing circum–North Atlantic ice sheets [*Clark et al*., 2002] and the Atlantic-to-Pacific moisture transport [*Broecker*, 1997; *Leduc et al*., 2007] are generally regarded as main drivers of the North Atlantic salt budget. However, mounting evidence also points to the salt transport through the Indian-Atlantic oceanic gateway (I-AOG), via the Agulhas Leakage, as a

Additional supporting information may be found in the online version of this article.

[1]Institut de Ciència i Tecnologia Ambientals, Universitat Autònoma de Barcelona, Cerdanyola del Vallès, Spain.
[2]Institució Catalana de Recerca i Estudis Avançats, Barcelona, Spain.
[3]Departament de Física, Universitat Autònoma de Barcelona, Cerdanyola del Vallès, Spain.
[4]School of Earth and Ocean Sciences, Cardiff University, Cardiff, UK.
[5]Alfred Wegener Institute, Bremerhaven, Germany.
[6]Earth & Climate Cluster Department of Earth Sciences, Faculty of Earth and Life Sciences, Vrije Universiteit Amsterdam, Amsterdam, Netherlands.
[7]Godwin Laboratory for Palaeoclimate Research, Department of Earth Sciences, University of Cambridge, Cambridge, UK.

Corresponding author: G. Marino, Institut de Ciència i Tecnologia Ambientals, Universitat Autònoma de Barcelona, 08193 Bellaterra, Cerdanyola del Vallès, Spain. (Gianluca.Marino@uab.cat)

0883-8305/13/10.1002/palo.20038

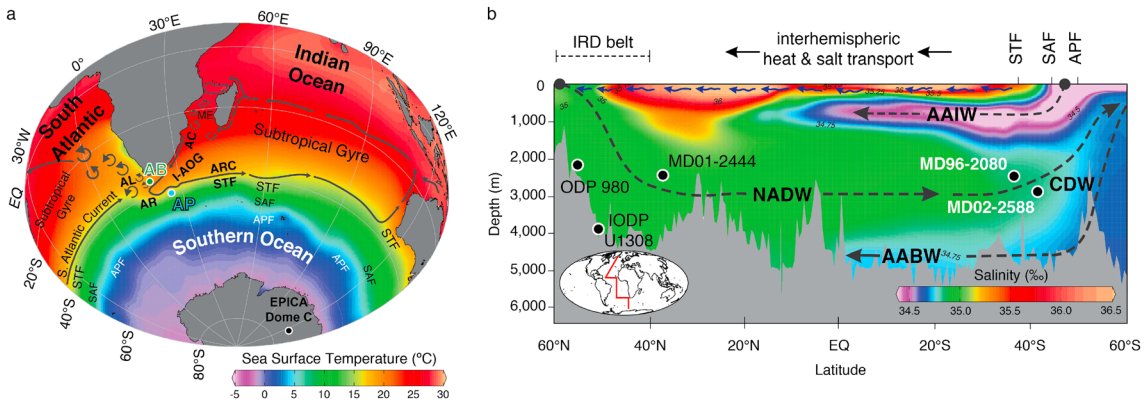

Figure 1. Location of sediment cores MD96-2080 and MD02-2588. (a) Map contours represent modern mean annual sea surface temperatures [*Schlitzer*, 2012] in the South Atlantic, South Indian, and Southern Oceans. Grey arrows indicate the main surface ocean circulation patterns with emphasis on the key components of the Indian-Atlantic oceanic gateway [*Lutjeharms*, 2006; *Beal et al*., 2011]. Green and cyan dots represent the locations of MD96-2080 (Agulhas Bank, AB) and MD02-2588 (Agulhas Plateau, AP), respectively. (b) Meridional cross section of seawater salinity through the Atlantic basin [*Schlitzer*, 2012] displaying the northward flowing thermocline waters (blue solid arrows) and the mean flow direction of North Atlantic Deep Water (NADW); Antarctic Intermediate Water (AAIW); Circumpolar Deep Water (CDW); and Antarctic Bottom Water (AABW). Figures 1a and 1b also display the Subtropical Front (STF); Subantarctic Front (SAF); and Antarctic Polar Front (APF). ME, Mozambique Channel Eddies; AC, Agulhas Current; AL, Agulhas Leakage; AR, Agulhas Retroflection; ARC, Agulhas Return Current; EPICA, European Project for Ice Coring in Antarctica.

likewise instrumental controlling factor [*Lutjeharms*, 2006; *Beal et al*., 2011]. The I-AOG currently "leaks" ~5–15 sverdrup (Sv, $10^6\,m^3\,s^{-1}$) of warm and saline Subtropical Indian Ocean water into the South Atlantic and is considered the dominant source of the upper branch of the AMOC, connecting the southern tip of Africa to the North Atlantic [*Gordon*, 1986; *Lutjeharms*, 2006; *Beal et al*., 2011].

[4] Paleoceanographic reconstructions of the I-AOG circulation are currently limited to orbital time scales [*Peeters et al*., 2004; *Martínez-Méndez et al*., 2010; *Caley et al*., 2012] and lack the temporal resolution and/or the paleoceanographic detail needed to decipher the potential connection between salt oscillations in the south and millennial-scale and abrupt AMOC and climate shifts. We present new and high-resolution paleoceanographic records from the western sector of the I-AOG (Figure 1), resolving a series of abrupt and high-amplitude surface ocean hydrographic (temperature and salinity) changes that recurred on a millennial time scale in the Agulhas Leakage area. These time series, which span the penultimate glacial-interglacial cycle (265–77 ka, Marine Isotope Stages, MIS, 8–5a) at multicentennial resolution, are discussed along with previously published records to explore the role of the Agulhas Leakage in the abrupt ocean and climate changes of the Late Pleistocene.

2. Materials and Methods

[5] Sediment cores MD96-2080 and MD02-2588 were retrieved with the RV *Marion Dufresne* from the Agulhas Bank and Agulhas Plateau, respectively (Figure 1). Core MD96-2080 (36°19.2′S, 19°28.2′E, 2488 m water depth) is ideally positioned to capture past changes in the Agulhas Leakage [*Lutjeharms*, 2006], and by focusing on penultimate climate cycle, we avoid a sedimentation gap in more recent sections of its sediment sequence [*Martínez-Méndez et al*., 2010]. Core MD02-2588 (41°19.9′S, 25°49.7′E, 2907 m water depth) is located close to the subtropical front (STF), which separates the warm subtropical waters of the eastward flowing Agulhas Return Current from the colder subantarctic waters to the south [*Lutjeharms*, 2006].

[6] We present a paired record ($N = 412$) of stable oxygen isotopes ($\delta^{18}O$) and magnesium-to-calcium ratios (Mg/Ca) for the planktic foraminifer *Globigerinoides ruber* (sensu stricto, white) along core MD96-2080. These profiles are complemented with Mg/Ca data ($N = 512$) for the planktic foraminifer *Globigerina bulloides* and ice-rafted detritus (IRD) counts ($N = 229$) in core MD02-2588.

2.1. Chronology

[7] The marine and ice core records used in this study were synchronized to a common time scale (see supporting information), using the Antarctic ice core chronologies [*Parrenin et al*., 2007; *Ruth et al*., 2007], which are tied to the new time scale constructed for the Greenland ice cores North Greenland Ice Core Project, North Greenland Eemian Ice Drilling [*Capron et al*., 2010; *Dahl-Jensen et al*., 2013] and are consistent with the time scale of the synthetic $\delta^{18}O_{ice}$ record of *Barker et al*. [2011].

2.2. Trace Element and Stable Oxygen Isotope Analyses in Planktic Foraminifera

[8] Sixty-five tests per sample for *G. ruber* (300–355 µm size fraction) and 55 for *G. bulloides* (250–315 µm size fraction) were picked, crushed between methanol-cleaned glass microscope slides, and subsequently mixed to homogenize them before splitting into two aliquots used for $\delta^{18}O$ and

trace element analyses. *G. ruber* is closely associated with the subtropical waters conveyed by the Agulhas Current to the tip of Africa [*Peeters et al*., 2004], and its data reflect the influence of the Agulhas Leakage on the hydrography of the Agulhas Bank more reliably than those derived from other foraminiferal species [e.g., *Martínez-Méndez et al*., 2010]. *G. bulloides* is ubiquitous in the South Atlantic [*Niebler and Gersonde*, 1998] and is adapted to the strong hydrographic gradients that are associated with the regional oceanic frontal systems, such as the STF in the vicinity of the Agulhas Plateau [*Lutjeharms*, 2006].

[9] Trace element analyses were carried out following standard cleaning procedures [*Barker et al*., 2003], complemented with the reductive step in core MD96-2080. Element ratios were determined by inductively coupled plasma-optical emission spectroscopy [*de Villiers et al*., 2002] and inductively coupled plasma-mass spectrometry [*Yu et al*., 2005] at the University of Cambridge and at the Universitat Autònoma de Barcelona. Long-term instrumental precision of element ratio data, determined by replicate analyses of standard solutions containing Mg/Ca = 1.3 mmol mol^{-1} (Cambridge) and Mg/Ca = 2.6 mmol mol^{-1} (Barcelona), was ±0.46% and ±1.30%, respectively. The accuracy of Mg/Ca determinations was confirmed by an interlaboratory study [*Greaves et al*., 2008]. The Mg/Ca data from I-AOG cores were tested for reproducibility by replicating ~20% of the records (see supporting information). Previously published calibrations [*Mashiotta et al*., 1999; *Anand et al*., 2003] were used to convert *G. ruber* and *G. bulloides* Mg/Ca values (Mg/Ca$_{G.\,ruber}$, Mg/Ca$_{G.\,bulloides}$) to calcification temperatures, which, due to the near-surface habitat of these species [*Hemleben et al*., 1989], approximate sea surface temperatures (SST) at the core sites.

[10] *G. ruber* $\delta^{18}O$ ($\delta^{18}O_{G.\,ruber}$) was determined at Cardiff University using a ThermoFinnigan MAT 252 mass spectrometer linked online to a single acid bath CarboKiel-II carbonate preparation device. External precision was better than ±0.08‰ (1σ). Isotope values are referred to the Vienna Peedee Belemnite scale through calibration to the NBS-19 carbonate standard.

2.3. Conversion of Paired Mg/Ca-$\delta^{18}O$ Data to Local Seawater $\delta^{18}O$

[11] The seawater $\delta^{18}O$ ($\delta^{18}O_{SW}$) record from core MD96-2080 is used as a proxy of past surface ocean salinity variations at the Agulhas Bank, building on the linear relationship between $\delta^{18}O_{SW}$ and salinity that is observed at the regional scale in the modern ocean [*LeGrande and Schmidt*, 2006]. We derive paleo-$\delta^{18}O_{SW}$ time series from paired Mg/Ca$_{G.\,ruber}$-$\delta^{18}O_{G.\,ruber}$ data (Figure S4, see also the supporting information for details on the analysis of uncertainties). The record of calcification temperature based on Mg/Ca$_{G.\,ruber}$ is used to correct $\delta^{18}O_{G.\,ruber}$ for the temperature-dependent (0.21 ± 0.01‰ °C^{-1}) water to carbonate $\delta^{18}O$ fractionation [*Bemis et al*., 1998]. Next, we subtract from the residual $\delta^{18}O_{SW}$ the mean ocean $\delta^{18}O_{SW}$, which reflects variations in global ice volume and obtain the local $\delta^{18}O_{SW}$. For this, sea level records [e.g., *Rohling et al*., 2009] are converted into mean ocean $\delta^{18}O_{SW}$ by assuming a ^{18}O enrichment of the global ocean by 0.008‰ per meter sea level lowering [*Schrag et al*., 2002].

2.4. Analyses of Ice-Rafted Detritus in Core MD02-2588

[12] Lithic fragments (IRD) were counted under a binocular microscope from the >150 μm size fraction, in order to limit interference by fine-grained terrigenous material stemming from non-ice rafting transport mechanisms (e.g., bottom currents) [*Teitler et al*., 2010]. Relatively large splits were counted to increase the likelihood that IRD occurring in low numbers appears in the results. The mineralogy of the IRD grains is mainly quartz, with some grains being feldspar or of mafic origin, and scanning electron microscope analysis reveals typical glacial microfeatures on the surface of the grains, such as grooves, deep troughs, linear steps, and chatter marks (Figure S5).

3. Results

[13] The $\delta^{18}O_{G.\,ruber}$ profile from the Agulhas Bank core MD96-2080 displays a clear glacial-interglacial modulation of the signal (Figure 2a), with glacial values that are heavier than interglacial ones by up to 1.4‰. Oscillations of $\delta^{18}O_{G.\,ruber}$ on a millennial time scale appear far less pronounced, generally in the order of 0.2‰ (see also Figure S6). By contrast, Mg/Ca$_{G.\,ruber}$ based SST and local $\delta^{18}O_{SW}$ profiles from the same site exhibit a prominent millennial-scale variability with abrupt increases by 2–5°C and 0.5–1.5‰, respectively, standing out as a series of distinct peaks (Figures 2b and 2c).

[14] Millennial-scale SST variability is only weakly expressed at the Agulhas Plateau core MD02-2588 (Figure 2d). This site is located near the southern border of the I-AOG (Figure 1) and is marginally influenced by the retroflected Agulhas waters which return to the Indian Ocean paralleling the STF [*Lutjeharms*, 2006; *Diz et al*., 2007]. Hence, the gradual and low amplitude warming shifts (slightly exceeding 1°C) that we observe are indicative of transient southward displacements of the STF. SST decreases by up to 2°C coincide with enhanced IRD deposition (Figure 2e), which testifies to episodes of pronounced northward advection of polar waters during circum-Antarctic cold phases [e.g., *Pahnke et al*., 2003], with the northward shift of the regional oceanic fronts supporting iceberg survivability as far north as ~41°S.

4. Discussion

4.1. Millennial-Scale Hydrographic Variability at the Tip of Africa

[15] Our results reveal that between MIS8 and MIS5 the surface ocean hydrography in the western sector of the I-AOG underwent a series of millennial-scale oscillations, which were particularly pronounced at the Agulhas Bank core site (Figures 2b–2e). The latitudinal migrations of the STF, inferred from the Agulhas Plateau SST and IRD records (Figures 2d and 2e), allude to changes in wind forcing associated with shifts of the Southern Hemisphere westerlies [*De Deckker et al*., 2012], with potential consequences for the surface circulation within the I-AOG and, in turn, for the leakage of warm and saline waters into the South Atlantic [*Lutjeharms*, 2006; *Beal et al*., 2011]. Indeed, the high-amplitude SST and $\delta^{18}O_{SW}$ increases observed at the Agulhas Bank (Figures 2b and 2c) testify to positive heat and salt anomalies during millennial-scale episodes of

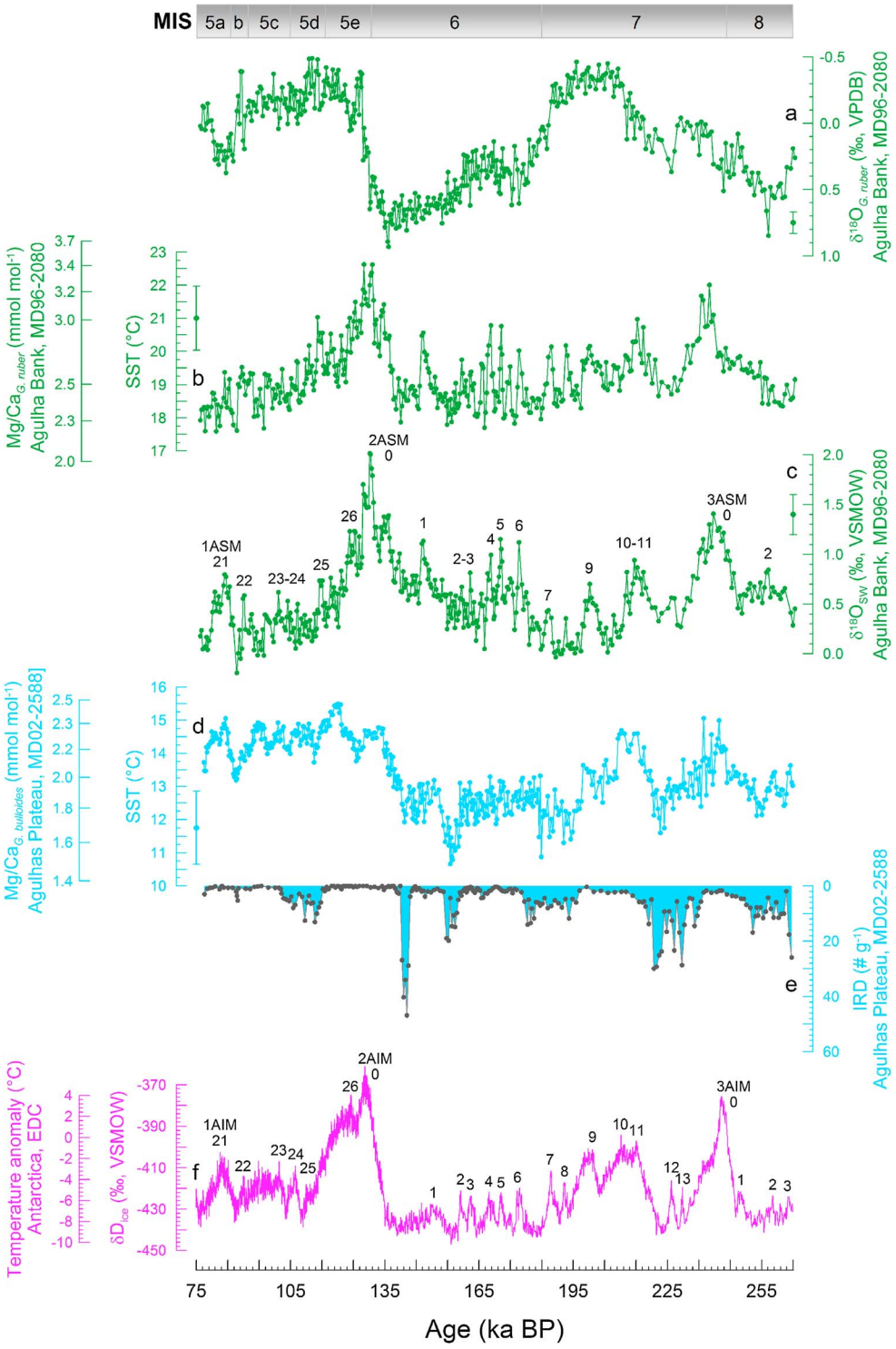

Figure 2. Agulhas Bank and Agulhas Plateau records of surface ocean variability. (a) $\delta^{18}O$ record for the planktic foraminifer *Globigerinoides ruber* (sensu stricto, white) in MD96-2080, Agulhas Bank. (b) *G. ruber* Mg/Ca results and calcification temperatures in MD96-2080, Agulhas Bank. (c) Ice volume corrected local $\delta^{18}O_{SW}$ record in MD96-2080, Agulhas Bank. (d) *Globigerina bulloides* Mg/Ca results and calcification temperatures in core MD02-2588, Agulhas Plateau. (e) Ice-rafted detritus (IRD) in MD02-2588, Agulhas Plateau (note inverse scale). (f) Antarctic δD_{ice} record of past atmospheric temperature changes from the European Project for Ice Coring in Antarctica (EPICA) Dome C [*Jouzel et al.*, 2007]. Each of the millennial-scale events in Figures 2c and 2b is identified by the climatic cycle to which it belongs and by a sequential number describing its position within the climatic cycle [cf. *Martrat et al.*, 2007]. MIS, Marine Isotopic Stage; ASM, Agulhas Salt-leakage Maximum; AIM, Antarctic Isotopic Maximum. Vertical error bars represent 1σ uncertainties.

southward migration of the STF. The Agulhas Bank is located directly in the path of the rings, eddies, and filaments constituting the Agulhas Leakage [*Lutjeharms*, 2006]. Accordingly, the $\delta^{18}O_{SW}$ and SST maxima at this site can be seen as hydrographic fingerprints of the enhanced transport to the southern tip of Africa of warm and saline waters, which are sourced in the subtropical Indian Ocean.

[16] The Agulhas Leakage feeds with heat and salt the upper branch of the AMOC that flows northward, compensating the formation and export of NADW to the Indian and Pacific Oceans [*Gordon*, 1986]. However, sustained heat loss to the atmosphere as the Agulhas waters exit the I-AOG causes the heat anomaly coupled with the leakage to dissipate [*Lutjeharms*, 2006], thereby amplifying the impact of salinity on the buoyancy of the waters advected to the South Atlantic and beyond [*Beal et al*., 2011]. In addition, both theoretical and numerical models hint at seawater salinity as the critical parameter that modulates millennial-scale buoyancy changes at the northern end of the AMOC's upper branch [*Broecker et al*., 1990; *Renold et al*., 2010]. Hence, in the following, we focus on the characteristics and large-scale implications of the Agulhas Bank $\delta^{18}O_{SW}$ oscillations. We identify 18 transient $\delta^{18}O_{SW}$ increases, dubbed Agulhas salt-leakage maxima (ASM), which are numerically coded on the basis of their correlation with the isotopic maxima in the Antarctic deuterium (δD_{ice}) record (Figure 2e). The most evident and long-lasting $\delta^{18}O_{SW}$ shifts display positive amplitudes of up to ~1.5‰ and mark the end of full glacial conditions of MIS8 and MIS6, corroborating the notion of a systematic deglacial strengthening of the Agulhas Leakage [*Peeters et al*., 2004; *Caley et al*., 2012]. However, $\delta^{18}O_{SW}$ fluctuations at the Agulhas Bank are not confined to glacial-interglacial transitions, large positive amplitude, but shorter-lasting events punctuate the glacial and interglacial sections alike (Figures 2 and 3). The significance of some of these $\delta^{18}O_{SW}$ anomalies (e.g., 1ASM23-24, 2ASM2-3) is equivocal as they remain within or barely exceed the bounds of the propagated (2σ) uncertainties, but in particular, during early MIS6 and MIS5a–b, their amplitudes are remarkably large, reaching up to two thirds of the major deglacial shifts.

4.2. Ocean-Atmosphere Interhemispheric Linkages

[17] The evidence of transient and high-amplitude oscillations in the Indian-to-Atlantic saltwater transport raises important questions concerning their relationship with the interhemispheric climate and AMOC dynamics on a millennial time scale. To explore such links, we place our I-AOG records into a framework of abrupt ocean-atmosphere changes from the wider North Atlantic region (Figures 3a–3f). Although the interhemispheric phasing discussed below is consistent with that identified in the nearby Cape Basin by *Charles et al*. [2010], the uncertainties (1σ, 0.4–1.3 kyr between 185 and 77 ka; Figure 3g) associated with our chronological framework hamper the clear identification of the timing of the ASM relative to their North Atlantic counterparts, at least for the short-lasting events. We consequently focus on the multimillennial ASM to build our interpretation and advance conceptual ideas concerning the I-AOG dynamics and its significance for interhemispheric teleconnections. Based on this data comparison, we note that the salinity buildup and peak maxima at the Agulhas Bank appear to correlate with millennial-scale cold phases and subsequent abrupt stadial-to-interstadial transitions documented in the Greenland air temperatures and in the Iberian Margin tetraunsaturated ($C_{37:4}$) alkenone profile from the Iberian Margin (Figures 3a and 3b). The latter traces the advection of cold surface Arctic waters to this region [*Martrat et al*., 2007]. These changes reflect the response of the circum–North Atlantic to AMOC variations [*Broecker et al*., 1990] coupled with ice sheet instabilities and attendant freshwater perturbation [*McManus et al*., 1999; *Oppo et al*., 2006].

[18] The prominent $\delta^{18}O_{SW}$ increase (1ASM21) at 87–84 ka is associated with the millennial-scale IRD pulse in the subpolar North Atlantic [*Oppo et al*., 2006] and with the incursion of surface Arctic waters to the Iberian Margin [*Martrat et al*., 2007]. This is a clear expression of the climate system's bipolar seesaw behavior, in which cooling (and freshening) in the North Atlantic coincides with warming over Antarctica [*Blunier and Brook*, 2001]. Other examples of ASM that correlated with abrupt swings in the north are as follows: (i) the 2ASM1 salt buildup at ~147 ka (Figure 3c); (ii) the double-peaked salinity increase between 138 and 130 ka, coinciding with Heinrich event 11 [*Oppo et al*., 2006]; (iii) the series of five consecutive ASM between ~158 and 181 ka (events 2ASM2–6); and (iv) the 1ASM22–25 salt events during MIS5. Events 2ASM2–6 also match the structure of the stadial-interstadial fluctuations in the Greenland $\delta^{18}O_{ice}$ composite, perhaps suggesting an interhemispheric coupling similar to that established above for the longer-lasting events during the penultimate deglaciation and 1ASM21.

[19] The curtailment of NADW (or its glacial equivalent) formation in response to positive surface buoyancy forcing during episodes of freshwater perturbation in the North Atlantic [e.g., *McManus et al*., 1999; *Clark et al*., 2002] has been shown to promote a basin-scale reconfiguration of the deep branch of the AMOC [*Renold et al*., 2010]. These changes are recorded as negative shifts in the stable carbon isotopes ($\delta^{13}C$) of bottom-dwelling foraminifera (Figure 3f) at Integrated Ocean Drilling Program Site U1308 [*Hodell et al*., 2008]. Site U1308 is well positioned (Figure 1b) to capture the northward incursions of nutrient-laden (low $\delta^{13}C$) southern component waters (equivalent to modern Antarctic bottom water) into the deep North Atlantic, which is otherwise ventilated by nutrient-depleted (high-$\delta^{13}C$) NADW [*Curry and Oppo*, 2005]. Numerical simulations show that the retention of oceanic heat in the south coupled with an AMOC slowdown [e.g., *Knutti et al*., 2004] is compensated by the intensification of the northward heat transport via the atmosphere [*Lee et al*., 2011], which ultimately weakens the Hadley Cell in the southern tropics and strengthens the midlatitude westerlies that shift toward Antarctica [*Toggweiler and Lea*, 2010; *Lee et al*., 2011]. This reconfiguration of the atmospheric circulation in the Southern Hemisphere potentially "drags" the STF to a southerly position [*De Deckker et al*., 2012], as exemplified by the surface ocean warming at the Agulhas Plateau (Figure 3d), and widens the I-AOG [*Beal et al*., 2011]. The latter would have then maximized the Agulhas Leakage into the South Atlantic, salinifying the surface ocean at the Agulhas Bank (Figure 3c). The resumption of NADW formation (Figure 3f) and of its associated heat piracy [*Knutti et al*., 2004] at the onset of interstadials (Figure 3a) would cause

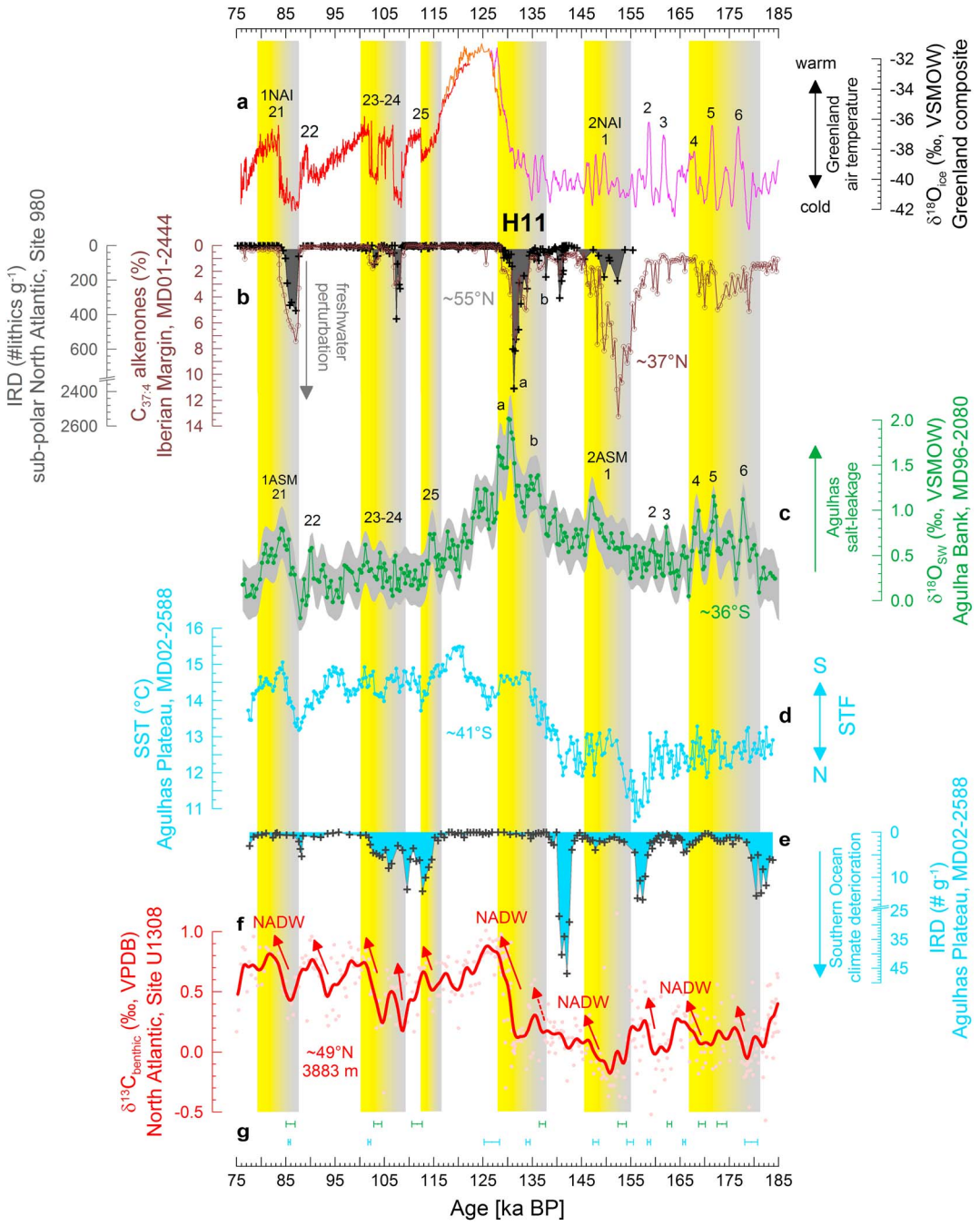

Figure 3. Linking Agulhas salt oscillations with ocean and climate changes in the North Atlantic. (a) Greenland $\delta^{18}O_{ice}$ composite [*Capron et al.*, 2010; *Barker et al.*, 2011; *Dahl-Jensen et al.*, 2013]. (b) Ice-rafted detritus (IRD, grey) from the subpolar North Atlantic, Ocean Drilling Program (ODP) Site 980 [*Oppo et al.*, 2006]. Tetraunsaturated alkenones ($C_{37:4}$) at the Iberian Margin [*Martrat et al.*, 2007]. (c) Agulhas Bank $\delta^{18}O_{SW}$ record. The shaded envelope illustrates the propagated 2σ uncertainty associated with the millennial-scale $\delta^{18}O_{SW}$ shifts discussed in the text. (d, e) Mg/Ca-derived (*G. bulloides*) SST and IRD from the Agulhas Plateau. (f) Benthic foraminiferal $\delta^{13}C$ profile [*Hodell et al.*, 2008] from the Integrated Ocean Drilling Program Site U1308 (North Atlantic, 3883 m water depth) with a 1 kyr Gaussian low-pass filter. (g) Tie points used to synchronize the MD02-2588 (cyan) and MD96-2080 (green) records to the EDC3/EDML1 chronology and associated 1σ uncertainties. NAI, North Atlantic Interstadials; ASM, Agulhas Salt-leakage Maximum; H11, Heinrich event 11.

this sequence of interhemispheric developments to reverse [*Toggweiler and Lea*, 2010; *Lee et al*., 2011]. Specifically, an equatorward migration of the STF over the Agulhas Plateau (Figures 3d and 3e) is expected to narrow the I-AOG and to hinder the Agulhas salt leakage to the South Atlantic, in line with the rapidly dissipating salinity anomalies at the Agulhas Bank (Figure 3c).

[20] Our analysis suggests that a dynamic connection between hydrographic changes in the I-AOG and in the North Atlantic climate is consistent with recently proposed adjustment processes of the coupled ocean-atmosphere system to a freshwater-bound weakening of the AMOC [*Knutti et al*., 2004; *Toggweiler and Lea*, 2010; *Lee et al*., 2011]. The salinity buildup in the Agulhas Leakage area during North Atlantic stadials, possibly superimposed upon an underlying salinification of the wider South Atlantic linked to AMOC weakening [*Lohmann*, 2003], may have had important implications for the buoyancy budget of the Atlantic Ocean and, in turn, for the AMOC [*Beal et al*., 2011]. It has been proposed that the salt sourced in the I-AOG and advected to the NADW formation sites has the potential to kick-start the AMOC [*Knorr and Lohmann*, 2003]. This raises the possibility that the Agulhas salt-leakage events that are documented in our records do not simply reflect a passive response of the I-AOG to the interhemispheric bipolar seesaw but either actively triggered the AMOC resumption or (at least) modulated its stability characteristics upon resumption [*Knorr and Lohmann*, 2007].

5. Concluding Remarks

[21] Results presented in this study indicate that transient and high-amplitude oscillations of the Agulhas salt leakage were a persistent feature of the I-AOG circulation in the past and were possibly dynamically linked with abrupt reorganizations of AMOC and interhemispheric climate. It emerges that the salt-leakage events at the southern tip of Africa occurred when the North Atlantic was cold and fresh (stadials) and the AMOC was weak and that the salt leakage maximized during the abrupt (stadial/interstadial) resumptions of the AMOC. This relationship involves the impact of changing AMOC strength and its coupled interhemispheric climate adjustment of the Southern Hemisphere westerlies, which plausibly altered the I-AOG circulation and impacted the Agulhas Leakage. Coupled climate models are needed to determine whether the salt leakage actively triggered the recovery of the AMOC from a perturbed state or it played a more passive role by contributing to the strengthening of the AMOC that was triggered elsewhere. The correlation of salt oscillations in the I-AOG and abrupt climate changes in the North Atlantic, however, poses a challenge to the canonical view ascribing abrupt climate swings exclusively to the processes taking place in the northern North Atlantic and/or in the Northern Tropics.

[22] **Acknowledgments.** L. Rodríguez-Sanz, M. Greaves, G. Mortyn, and C. Lear provided analytical advice. I. Villarroya, C. Cantero, and J. Becker assisted during geochemical analyses. G. Martínez-Méndez, F. Peeters, J.R. Toggweiler, and C. Charles (Editor) are acknowledged for their constructive comments that helped improve the manuscript. We thank L. Rodríguez-Sanz for her advice on the statistical analysis of the data. Financial support was provided by the Universitat Autònoma de Barcelona (grant PS-688-01/08) to G.M., by the European Commission Seventh Framework Programme (EC FP7) collaborative project "Past4Future" (G.M., P.Z., R.Z.), by the EC FP7 Initial Training Network "GATEWAYS" (C.P.P., I.H., G.K., G.M., M.Z., P.Z., R.Z.), by the Natural Environment Research Council, UK (I.H., H.E.), by the European Research Council (grant 2010-NEWLOG ADG-267931, H.E.), and by the Helmholtz Climate Initiative "Regional Climate Change" (REKLIM, G.K.).

References

Anand, P., H. Elderfield, and M. H. Conte (2003), Calibration of Mg/Ca thermometry in planktonic foraminifera from a sediment trap time series, *Paleoceanography*, *18*(2), 1050, doi:10.1029/2002PA000846.

Barker, S., M. Greaves, and H. Elderfield (2003), A study of cleaning procedures used for foraminiferal Mg/Ca paleothermometry, *Geochem. Geophys. Geosyst.*, *4*(9), 8407, doi:10.1029/2003GC000559.

Barker, S., G. Knorr, R. L. Edwards, F. Parrenin, A. E. Putnam, L. C. Skinner, E. Wolff, and M. Ziegler (2011), 800,000 years of abrupt climate variability, *Science*, *334*(6054), 347–351.

Beal, L. M., W. P. M. De Ruijter, A. Biastoch, and R. Zahn (2011), On the role of the Agulhas system in ocean circulation and climate, *Nature*, *472*(7344), 429–436.

Bemis, B. E., H. J. Spero, J. Bijma, and D. W. Lea (1998), Reevaluation of the oxygen isotopic composition of planktonic foraminifera: Experimental results and revised paleotemperature equations, *Paleoceanography*, *13*(2), 150–160.

Blunier, T., and E. J. Brook (2001), Timing of millennial-scale climate change in Antarctica and Greenland during the last glacial period, *Science*, *291*(5501), 109–112.

Broecker, W. S. (1997), Thermohaline circulation, the Achilles heel of our climate system: Will man-made CO_2 upset the current balance?, *Science*, *278*(5343), 1582–1588.

Broecker, W. S. (1998), Paleocean circulation during the last deglaciation: A bipolar seesaw?, *Paleoceanography*, *13*(2), 119–121.

Broecker, W. S., G. Bond, M. Klas, G. Bonani, and W. Wolfli (1990), A salt oscillator in the glacial Atalntic? 1. The concept, *Paleoceanography*, *5*(4), 469–477.

Caley, T., J. Giraudeau, B. Malaizé, L. Rossignol, and C. Pierre (2012), Agulhas leakage as a key process in the modes of Quaternary climate changes, *Proc. Natl. Acad. Sci.*, *109*(18), 6835–6839.

Capron, E., et al. (2010), Synchronising EDML and NorthGRIP ice cores using $\delta^{18}O$ of atmospheric oxygen ($\delta^{18}O_{atm}$) and CH_4 measurements over MIS5 (80–123 kyr), *Quat. Sci. Rev.*, *29*(1–2), 222–234.

Charles, C. D., K. Pahnke, R. Zahn, P. G. Mortyn, U. Ninnemann, and D. A. Hodell (2010), Millennial scale evolution of the Southern Ocean chemical divide, *Quat. Sci. Rev.*, *29*(3–4), 399–409.

Cheng, H., R. L. Edwards, W. S. Broecker, G. H. Denton, X. Kong, Y. Wang, R. Zhang, and X. Wang (2009), Ice Age terminations, *Science*, *326*(5950), 248–252.

Clark, P. U., N. G. Pisias, T. F. Stocker, and A. J. Weaver (2002), The role of the thermohaline circulation in abrupt climate change, *Nature*, *415*(6874), 863–869.

Curry, W. B., and D. W. Oppo (2005), Glacial water mass geometry and the distribution of $\delta^{13}C$ of CO_2 in the western Atlantic Ocean, *Paleoceanography*, *20*, PA1017, doi:10.1029/2004PA001021.

Dahl-Jensen, D., et al. (2013), Eemian interglacial reconstructed from a Greenland folded ice core, *Nature*, *493*(7433), 489–494.

De Deckker, P., M. Moros, K. Perner, and E. Jansen (2012), Influence of the tropics and southern westerlies on glacial interhemispheric asymmetry, *Nat. Geosci.*, *5*(4), 266–269.

de Villiers, S., M. Greaves, and H. Elderfield (2002), An intensity ratio calibration method for the accurate determination of Mg/Ca and Sr/Ca of marine carbonates by ICP-AES, *Geochem. Geophys. Geosyst.*, *3*(1), 1001, doi:10.1029/2001GC000169.

Diz, P., I. R. Hall, R. Zahn, and E. G. Molyneux (2007), Paleoceanography of the southern Agulhas Plateau during the last 150 ka: Inferences from benthic foraminiferal assemblages and multispecies epifaunal carbon isotopes, *Paleoceanography*, *22*, PA4218, doi:10.1029/2007PA001511.

Gordon, A. L. (1986), Inter-ocean exchange of thermocline water, *J. Geophys. Res.*, *91*(C4), 5037–5046.

Greaves, M., et al. (2008), Interlaboratory comparison study of calibration standards for foraminiferal Mg/Ca thermometry, *Geochem. Geophys. Geosyst.*, *9*, Q08010, doi:10.1029/2008GC001974.

Hemleben, C., M. Spindler, and O. R. Anderson (1989), *Modern Planktonic Foraminifera*, Springer-Verlag, New York.

Hodell, D. A., J. E. T. Channell, J. H. Curtis, O. E. Romero, and U. Roehl (2008), Onset of "Hudson Strait" Heinrich events in the eastern North Atlantic at the end of the middle Pleistocene transition (~640 ka)?, *Paleoceanography*, *23*, PA4218, doi:10.1029/2008PA001591.

Jouzel, J., et al. (2007), Orbital and millennial Antarctic climate variability over the past 800,000 years, *Science*, *317*(5839), 793–796.

Knorr, G., and G. Lohmann (2003), Southern Ocean origin for the resumption of Atlantic thermohaline circulation during deglaciation, *Nature*, *424*(6948), 532–536.

Knorr, G., and G. Lohmann (2007), Rapid transitions in the Atlantic thermohaline circulation triggered by global warming and meltwater during the last deglaciation, *Geochem. Geophys. Geosyst.*, *8*, Q12006, doi:10.1029/2007GC001604.

Knutti, R., J. Flückiger, T. F. Stocker, and A. Timmermann (2004), Strong hemispheric coupling of glacial climate through freshwater discharge and ocean circulation, *Nature*, *430*(7002), 851–856.

Leduc, G., L. Vidal, K. Tachikawa, F. Rostek, C. Sonzogni, L. Beaufort, and E. Bard (2007), Moisture transport across Central America as a positive feedback on abrupt climatic changes, *Nature*, *445*(7130), 908–911.

Lee, S.-Y., J. C. H. Chiang, K. Matsumoto, and K. S. Tokos (2011), Southern Ocean wind response to North Atlantic cooling and the rise in atmospheric CO_2: Modeling perspective and paleoceanographic implications, *Paleoceanography*, *26*, PA1214, doi:10.1029/2010PA002004.

LeGrande, A. N., and G. A. Schmidt (2006), Global gridded data set of the oxygen isotopic composition in seawater, *Geophys. Res. Lett.*, *33*, L12604, doi:10.1029/2006GL026011.

Lohmann, G. (2003), Atmospheric and oceanic freshwater transport during weak Atlantic overturning circulation, *Tellus, Ser. A*, *55*(5), 438–449.

Lutjeharms, J. R. E. (2006), *The Agulhas Current*, 329 pp., Springer, Berlin.

Martínez-Méndez, G., R. Zahn, I. R. Hall, F. J. C. Peeters, L. D. Pena, I. Cacho, and C. Negre (2010), Contrasting multiproxy reconstructions of surface ocean hydrography in the Agulhas Corridor and implications for the Agulhas Leakage during the last 345,000 years, *Paleoceanography*, *25*, PA4227, doi:10.1029/2009PA001879.

Martrat, B., J. O. Grimalt, N. J. Shackleton, L. de Abreu, M. A. Hutterli, and T. F. Stocker (2007), Four climate cycles of recurring deep and surface water destabilizations on the Iberian margin, *Science*, *317*(5837), 502–507.

Mashiotta, T. A., D. W. Lea, and H. J. Spero (1999), Glacial-interglacial changes in Subantarctic sea surface temperature and δ^{18}O-water using foraminiferal Mg, *Earth Planet. Sci. Lett.*, *170*(4), 417–432.

McManus, J. F., D. W. Oppo, and J. L. Cullen (1999), A 0.5-million-year record of millennial-scale climate variability in the North Atlantic, *Science*, *283*(5404), 971–975.

Niebler, H. S., and R. Gersonde (1998), A planktic foraminiferal transfer function for the southern South Atlantic Ocean, *Mar. Micropaleontology*, *34*(3–4), 213–234.

Oppo, D. W., J. F. McManus, and J. L. Cullen (2006), Evolution and demise of the Last Interglacial warmth in the subpolar North Atlantic, *Quat. Sci. Rev.*, *25*(23–24), 3268–3277.

Pahnke, K., R. Zahn, H. Elderfield, and M. Schulz (2003), 340,000-year centennial-scale marine record of Southern Hemisphere climatic oscillation, *Science*, *301*(5635), 948–952.

Parrenin, F., et al. (2007), The EDC3 chronology for the EPICA dome C ice core, *Clim. Past.*, *3*(3), 485–497.

Peeters, F. J. C., R. Acheson, G. J. A. Brummer, W. P. M. de Ruijter, R. R. Schneider, G. M. Ganssen, E. Ufkes, and D. Kroon (2004), Vigorous exchange between the Indian and Atlantic oceans at the end of the past five glacial periods, *Nature*, *430*(7000), 661–665.

Renold, M., C. C. Raible, M. Yoshimori, and T. F. Stocker (2010), Simulated resumption of the North Atlantic meridional overturning circulation—Slow basin-wide advection and abrupt local convection, *Quat. Sci. Rev.*, *29*(1–2), 101–112.

Rohling, E. J., K. Grant, M. Bolshaw, A. P. Roberts, M. Siddall, C. Hemleben, and M. Kucera (2009), Antarctic temperature and global sea level closely coupled over the past five glacial cycles, *Nat. Geosci.*, *2*(7), 500–504.

Ruth, U., et al. (2007), "EDML1": a chronology for the EPICA deep ice core from Dronning Maud Land, Antarctica, over the last 150 000 years, *Clim. Past.*, *3*(3), 475–484.

Schlitzer, R. (2012), Ocean data view, edited.

Schrag, D. P., J. F. Adkins, K. McIntyre, J. L. Alexander, D. A. Hodell, C. D. Charles, and J. F. McManus (2002), The oxygen isotopic composition of seawater during the Last Glacial Maximum, *Quat. Sci. Rev.*, *21*(1–3), 331–342.

Teitler, L., D. A. Warnke, K. A. Venz, D. A. Hodell, S. Becquey, R. Gersonde, and W. Teitler (2010), Determination of Antarctic Ice Sheet stability over the last similar to 500 ka through a study of iceberg-rafted debris, *Paleoceanography*, *25*, PA1202, doi:10.1029/2008PA001691.

Toggweiler, J. R., and D. W. Lea (2010), Temperature differences between the hemispheres and ice age climate variability, *Paleoceanography*, *25*, PA2212, doi:10.1029/2009PA001758.

Trenberth, K. E., and J. M. Caron (2001), Estimates of meridional atmosphere and ocean heat transports, *J. Climate*, *14*(16), 3433–3443.

Yu, J. M., J. Day, M. Greaves, and H. Elderfield (2005), Determination of multiple element/calcium ratios in foraminiferal calcite by quadrupole ICP-MS, *Geochem. Geophys. Geosyst.*, *6*, Q08P01, doi:10.1029/2005GC000964.